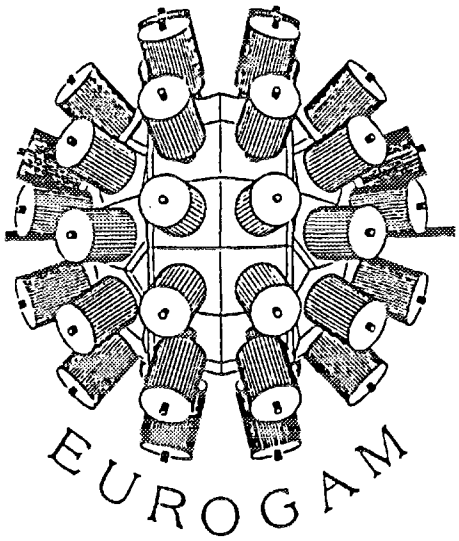

FRANCE - UK

Collaboration

CRN 95-08

Ballistic Deficit Correction Methods For Large Ge Detectors-High Counting Rate Study

G.Duchêne and M.Moszyński*

* Soltan Institute for Nuclear Studies, PL05-400, Świerk-Otwock, Poland

Submitted to Nuclear Instr. Meth.

CENTRE DE RECHERCHES NUCLEAIRES
STRASBOURG

IN2P3
CNRS

UNIVERSITE
LOUIS PASTEUR

BALLISTIC DEFICIT CORRECTION METHODS FOR LARGE Ge DETECTORS- HIGH COUNTING RATE STUDY

G.Duchêne and M.Moszyński *

Centre de Recherches Nucléaires, IN2P3-CNRS/Université Louis Pasteur, BP 28, F 67037 Strasbourg Cedex 2, France

Abstract

A comparative study is carried out for different ballistic deficit correction methods versus input count rate (from 3 to 50 kcounts/s) using four large Ge detectors of about 70 % relative efficiency. The present work shows that, at shaping time constants shorter or equal to 2 μs, the Tennelec TC245 linear amplifier in the BDC mode (Hinshaw method) is the best compromise for energy resolution and throughput. At low and moderate input count rates ($\leq$ 10 kcounts/s) the Ortec 675 Ge resolution enhancer based on the Goulding/Landis method offers excellent energy resolution and throughput at 2 μs shaping time. The energy resolution obtained with the Intertechnique 7201 gated integrator is very sensitive to count rate which lowers the interest in this module. At 3 kcounts/s it works very satisfactorily. All correction methods lead to narrow sum-peaks indistinguishable from single γ lines. More than the classical throughput, the full energy peak throughput is found representative of the pile-up inspection dead time of the corrector circuits. A new synthetic representation, plotting simultaneously energy resolution and throughput versus input count rate, is proposed.

*On leave of absence from Soltan Institute for Nuclear Studies, PL05-400, Świerk-Otwock, Poland (present address)

1. Introduction

A new generation of Ge multidetector arrays has been developed in different countries: Eurogam [1] in the U.K. and France, GASP [2] in Italy, Gammasphere [3] in the U.S.A. and finally Euroball [4], a large European collaboration. The goal for the designers is to obtain simultaneously a large photopeak detection efficiency for the whole array, with a reduced dead time (pile-up), good peak-to-background ratio and good energy resolution. The large efficiency has been reached by using large volume Ge detectors (relative efficiency larger than 70 %) surrounded by very compact BGO anti-Compton shields allowing a close packing of the Ge-BGO spectrometers around the target. Even more compact geometries are obtained using composite Ge detectors like the Clover detector in Eurogam [1] and the Cluster detector in Euroball [4]. The Ge-BGO spectrometers lead to excellent peak-to-background ratios. The use of new integrated electronics [5] shortening the encoding and the readout of the data reduces the dead time per nuclear event to 15 μs [5] especially if short shaping time constants are implemented in the linear amplifier (1.8 μs for Eurogam electronics). However, as the charge collection time of the carriers depends strongly on the radial position where a γ-ray has been detected in the large Ge crystal [6], the energy resolution of the Ge detector deteriorates when short shaping time constants are used. Thus, the application of ballistic deficit correctors assures simultaneously a good energy resolution and a low pile-up rate which are important in multifold coincidence experiments. Furthermore large count rates are now reachable with such electronics.

In a previous paper [7] three different ballistic deficit correction methods applied to the spectroscopy amplifier output pulse with Gaussian shaping were compared for the gated integrator (GI) used by the Intertechnique 7201 module and the Ortec 973 high rate amplifier, the Hinshaw method [8] applied to the Tennelec TC245 amplifier and the Goulding/Landis method [9] generalised by Simpson et al. [10] and implemented on the Ortec 675 Ge resolution enhancer. Since this study was addressed mainly to the basic comparison of the different ballistic deficit correction methods, all the measurements were performed at low count rate, about 3000 counts/s, to avoid any influence on the data of the particular technical design of the electronics modules. The data analysis showed that at low count rate the

best energy resolution for both high and low γ-ray energies is achieved for short shaping time constants ($\leq 1\mu$s) with the gated integrators and for longer shaping time constants ($\geq 2\mu$s) with the Ortec 675 Ge resolution enhancer.

A full comparison of the different correction methods needs however to take into account their high count rate characteristics, e.g. the dependency of Ge energy resolution versus count rate and throughput. Since the results are in fact very sensitive to the specific technical design of the tested electronics modules, such analysis is also a test of the different technical realisations.

The aim of this work is to study the count rate performances of the Tennelec TC245 spectroscopy amplifier together with different ballistic deficit correctors as the Hinshaw method directly implemented in the TC245 module (BDC mode), the Intertechnique 7201 gated integrator and the Ortec 675 Ge resolution enhancer. The results of the measurements are compared to those obtained with the spectroscopy amplifier itself using the triangular shaping (TC245 module in standard mode).

All the measurements were carried out with short shaping time constants ranging from 0.5 to 2 μs.

2. Experimental details

2.1. Detectors

All the measurements were performed with four Ge detectors of 70-80 % relative efficiency presenting a coaxial tapered shape [1]. The detectors used were delivered by Ortec to the Eurogam collaboration. The technical characteristics of the detectors according to the manufacturer are specified in table 1.

2.2. Electronics

The study has been carried out with the different ballistic deficit correctors discussed in sect.1. Reference spectra were measured using the Tennelec TC245 amplifier with triangular shaping. The combination of the electronics modules and shaping time constants are summarized in table 2. As the present study is focussed on high count rates, the shaping time constants have been deliberately limited to values smaller or equal to 2 μs. Note that the use of the spectroscopy amplifier

alone with a shaping time constant of 0.5 μs leads to very poor energy resolutions of about 15 keV. The Ortec 675 Ge resolution enhancer is also quite ineffective for shaping time constants shorter than 2 μs [7]. Therefore such measurements have not been performed in the present work. Finally, the shaping time constants of the Intertechnique 7201 gated integrator are limited to the range 0.25 μs to 1 μs.

2.3. Method

All the measurements were carried out for count rates ranging from 3000 to 50000 counts/s. The number of detected γ-rays, N_{IN}, were measured by counting the ICR pulses delivered by TC245 amplifier using a scaler. Energy spectra were recorded by the Nucleus multichannel analyser based on an IBM PC. The energy resolution was determined directly by the analyser.

The measurements of ^{60}Co spectra were performed with an energy calibration of about 0.33 keV/channel. To increase the accuracy of the quoted energy resolution every measurement was repeated three times and the corresponding mean value was used for the discussion. The accuracy of a single measurement is 0.17 keV which leads to an uncertainty of 0.10 keV for the average values.

To determine the throughput characteristics of the studied spectroscopy modules two quantities were measured: the input and output number of counts respectively N_{IN} and N_{OUT}. Concerning the output rate, the number of counts N_{OUT} at the output of the ballistic deficit correctors, or, for the amplifier alone, the number of counts at the output of the stretcher built in the TC245 module (with pile-up rejector switched off) was measured by means of a scaler with a threshold set just above the noise.

Another quantity which characterizes the throughput is the number of counts N_P under the 1.33 MeV full energy peak measured by the multichannel analyser for a given live time.

Note that in respect to throughput the different electronics modules are not equivalent. The simple spectroscopy amplifier is not controlled by a pile-up rejector whereas the other modules use built in pile-up rejectors which control the output pulses. Thus the throughput characteristics of each ballistic deficit corrector are in fact controlled by the type of pile-up rejector chosen by the electronics manufacturer.

3. Results

3.1. Energy resolution study

3.1.1. Comparison of the methods

Fig.1 compares the 1.33 MeV ^{60}Co full energy peak measured at 3000 counts/s and at 50000 counts/s with the different electronics modules listed in table 2 and with Ge 40219 which presents very good intrinsic characteristics (see table 1). The y-scale is logarithmic.

At 2 μs shaping time constants, the TC245 amplifier alone (in fig.1a) leads to slightly asymmetric peaks with the quite good energy resolutions of 2.31 keV and 2.50 keV at respectively 3000 counts/s and 50000 counts/s. Applying a ballistic deficit correction by use of the TC245 amplifier in the BDC mode (fig.1b) or Ortec 675 Ge resolution enhancer (fig.1c), the energy resolution is improved by about 0.2-0.4 keV at low count rate and 0.1-0.4 keV at high count rate. The best results are obtained with the Ortec 675 module. Indeed the peak after correction is very symmetrical and its width is insensitive to count rate: the energy resolution of 1.93 keV at 3000 counts/s slowly moves to 2.07 keV at 50000 counts/s. These measurements, however, were performed with a 2 μs shaping time constant for which the throughput is rather poor (see sect. 3.2.). Thus we compare the BDC mode of the TC245 amplifier (fig.1d) and the Intertechnique 7201 gated integrator GI (fig.1e) at 1 μs shaping time constants. Both modules lead to almost the same quality energy spectra and present improved energy resolutions at low count rate and equivalent data at high count rate as the TC245 amplifier alone at 2 μs shaping time constant. Therefore throughput has to be taken into account to finally compare, the two correction methods (see sect.3.2.).

Fig.2 summarizes the energy resolution values measured with detector 40219 versus count rate for different ballistic deficit correctors and different shaping time constants.

At 2 μs shaping time the Ortec 675 Ge resolution enhancer assures a very good resolution at low count rate due to compensation of both ballistic deficit and trapping effects (stars in fig.2). Up to 5000 counts/s the FWHM after correction is even better than the value specified by the manufacturer and measured at 6

μs shaping time. The Goulding/Landis method (Ortec 675 unit) is by far more powerful than the Hinshaw method (TC245 module in BDC mode; full circles in fig.2). This is particularly visible at high count rate where the resolution obtained with TC245 BDC is about 0.3 keV worse. In fact the FWHM measured with the Ortec 675 module shows a quite flat evolution versus count rate which suggests that the ballistic deficit correction based on the measurement of the peaking time of the amplifier pulse is little affected by this parameter. It is also interesting to note that the variation versus count rate of the FWHM obtained with the TC245 amplifier alone is more pronounced then for the Ortec 675 unit which therefore may even compensate the distortions introduced by the amplifier itself.

Concerning the Hinshaw method, the deterioration at 2 μs shaping time of the energy resolution versus count rate is more pronounced for the TC245 amplifier in the BDC mode (full circles in fig.2) than in the standard mode (triangles in fig.2). As the output signal in BDC mode results from both unipolar and bipolar pulses which are similarly affected by the count rate, the TC245 amplifier in the BDC mode shows poorer performances versus count rate than the amplifier alone.

The comparison of the Intertechnique 7201 gated integrator GI (diamonds) and Tennelec TC245 BDC at 1 μs shaping time (full circles) shows that the gated integrator is more sensitive to count rate (fig.2). As mentioned in ref. [7], the gated integrator assures better energy resolution at low count rate. At higher rates however, the FWHM start to be comparable or even worse than the resolutions obtained with TC245 BDC. This effect is particularly pronounced at 0.5 μs shaping time. It is known that gated integrators are sensitive to baseline fluctuations. Their reduction requires a high precision pole zero cancellation which in turn is also controlled by the quality of the output signal from the preamplifier.

At this point, we would like to mention an interesting phenomenon observed in the energy spectra measured with the ballistic deficit correction at high count rates.

It is well known that the accidental photopeak detection of two γ-rays during the pulse processing time of the amplifier leads to a sum-peak in the energy spectrum which is more pronounced when a pile-up rejector is used. This is shown in fig.3 where the 662 keV ^{137}Cs full energy peak is on the left-hand part of the figure and the corresponding sum-peak on the right-hand side. In fig.3a the mea-

surement was done with the TC245 amplifier in the standard mode with a 2 μs shaping time, at a count rate of 37000 counts/s and without pile-up rejection. Fig.3b presents the same spectra with the pile-up rejector switched on. In the region of the sum-peak one observes a bump which is clearly evidenced when the pile-up rejection is active. Its energy resolution is equal to 4.1 keV. Fig.3c represents the same spectra measured with TC245 in the BDC mode. First of all, note the satellite peaks above the 662 keV ^{137}Cs full energy peak which were identified as sum-peaks of the 662 keV gamma-ray and the K and L X rays from ^{137}Cs. On the right-hand side of the figure one observes a well defined sum-peak at 1324 keV with an excellent energy resolution of 2.09 keV. It is not possible to distinguish such true sum peaks from these due to the detection of single γ-rays. The intensity of the sum-peak relative to the intensity of the 662 keV gamma line is 0.5 %. The observed effect shows that the BDC circuit does not distinguish between regular slow rising pulses and those built of two independent pulses summed within the dead time of the pile-up rejector. This points out the effectiveness of BDC circuit which, on the other hand, will complicate the analysis of high-rate γ spectra. Note that the same effect on sum peaks is observed with the Intertechnique 7201 gated integrator and the Ortec 675 Ge resolution enhancer.

The above comparison of the different ballistic deficit correctors shows that the best energy resolution performances are achieved with Ortec 675 Ge resolution enhancer at 2 μs shaping time which however limits the high count rate applications. The Tennelec TC245 BDC and Intertechnique 7201 gated integrator are comparable with respect to energy resolution although the energy resolution measured with the latter deteriorates more rapidly with count rate. Thus a full comparison between these two modules has also to include a throughput performance analysis.

3.1.2. Comparison of the detectors

The four Ortec Ge detectors used to perform the present study are designated as follows: 30526, 40219, 40187 and 40228. Their technical characteristics given by the manufacturer and summarized in table 1 show that the four counters are roughly equivalent and exhibit excellent performance for the size of their crystals.

A more detailed comparison among the different detectors is shown in fig.4 which presents the Ge detector energy resolution versus count rate for all the

counters for different electronics modules (see table 2).

As a general trend, two detectors 40219 (full squares) and 40228 (open diamonds) give similar energy resolutions over the whole count rate range at 1 and 2 μs with the different electronics modules. These two counters are the best of the Ge pool. Their good FWHM at low count rate is weakly affected by high count rate except for the gated integrator. The about 0.2 keV improvement of their energy resolution at 2 μs shaping time between triangular and BDC mode reflects the ballistic deficit compensation. The further improvement of about 0.1 keV using the Ortec 675 is more related to the carrier trapping corection. Both detectors work with the highest bias voltages of the Ge pool, - 4000 V or more (see Table 1).

In contrast, the detector 40187 (open stars) presents different characteristics. At 1 μs shaping time using TC245 in the standard mode (triangular shaping) its energy resolution of 4.5 keV is by about 1 keV worse than the resolution of the other detectors. At 2 μs shaping and for count rates smaller than 30 000 counts/s, the 40187 detector also exhibits the most deteriorated energy resolution. The TC245BDC compensates ballistic deficit by about 0.3 keV at 2 μs shaping but the FWHM measured is still worse compared to the data obtained with the counters 40219 and 40228. The energy resolution of counter 40187 improves to the same level as the reference detectors only using Ortec 675 Ge resolution enhancer. These observations suggest that the detector 40187 exhibits a large contribution of both ballistic deficit and majority carrier trapping effects. To better understand this effect one can refer to table 1 that presents the characteristics of the detectors. It shows that the 40187 detector works with the lowest bias voltage (-3000 V) and has the largest diameter (77.7 mm) of the Ge pool. This may lead to a relatively low electric field in the external region of the crystal which evidently increases the ballistic deficit and makes trapping more probable.

The detector 30526 (full circles) is characterised by the best energy resolution of the four detectors at low count rate, as measured with the amplifier alone at 1 μs shaping. This suggests a fast charge collection process, weakly affected by trapping. This seems to be confirmed by two observations:

- at 2 μs shaping time the energy resolution is weakly improved (by $\sim$0.1

keV) by the TC245 BDC compared to triangular shaping which shows a small contribution of ballistic deficit at this shaping.

- the 30526 is the only detector whose energy resolution is not improved at low count rate by the use of the Ortec 675 Ge resolution enhancer.

The latter point suggests an exceptionally weak contribution of the majority carrier trapping. However, the energy resolutions of 30526 measured with the Ortec 675 unit are significantly worse than those obtained with the other detectors indicating that this deterioration originates from another effect.

At high count rate the detector 30526 represents the worst case. Its energy resolution measured with the different electronic modules varies strongly with count rate (fig.4). Even the measurements made with the 675 unit are seriously affected. To better understand this behaviour fig.5 displays the shape of the 1.33 MeV ^{60}Co full energy peak measured with the TC245 in the BDC mode with 2 μs shaping.

At 3000 counts/s the peak shows a regular gaussian shape with an energy resolution of 2.29 keV (fig.5a). The same peak at 50000 counts/s exhibits a long high energy tail and an energy resolution of 2.87 keV (fig.5b). The intensity of the tailing is significantly increased when the detector is irradiated from the side and the energy resolution moves to 3.16 keV (fig.5c). The same effect was observed with the other modules. Inspection of the amplifier output pulse by means of an oscilloscope showed that behind most of the triangular pulses there was a long positive tail not compensated for by means of the pole-zero cancellation. This implies that the above effect is generated by another process in the detector. The more pronounced high-energy tail of the full energy peak under side irradiation suggests the existence of a dead layer at the external surface of the detector with a very weak electric field. This is confirmed by table 1 were the characteristics of the detectors 30526 and 40219 are compared. Though the crystal lengths are identical for both counters the diameter of 30526 is larger by 1.4 mm, and its relative efficiency is smaller by 5 %. Moreover, this detector which shows a small ballistic deficit and a weak carrier trapping (fig.4) has the worst peak shape of the Ge pool (1.97) and the smallest peak-to-Compton ratio (70.4). Finally, we have performed a lateral scanning of the crystal with a collimated ^{241}Am source which

revealed an external dead layer starting in the middle of the crystal length and extending to its rear side with a thickness varying between 3 and 7 mm. It has been checked that this inactive volume is present around the total circumference of the crystal.

In the above discussion, we have shown for crystal 30526 that its small ballistic deficit is compensated by the TC245 BDC and that the majority carrier trapping effect is negligible. This raises an important question:

- is this small carrier trapping related to the existence of the external dead layer ?

This could suggest that most of trapping centers are created close to the external surface of the crystal during a contact preparation process or surface treatment.

The above comparison of detector performances at high count rate demonstrates that for γ spectroscopy applications and large multidetector arrays it is not sufficient to characterise Ge counters only by the energy resolution measured with $6\mu s$ shaping time at 1000 counts/s. Other tests reflecting the properties of the detectors at high count rate like sensitivity of the energy resolution versus count rate with or without different ballistic deficit correction methods should be carried out. Moreover a high bias voltage above -4000 V is required for large Ge detectors in high count rate measurements.

3.2. Throughput

3.2.1. Comparison of the methods

To determine the throughput performance of different ballistic deficit correctors two quantities were measured versus the number of input pulses N_{IN}: the number of pulses N_{OUT} at the output of the ballistic corrector circuit and the number of counts N_{PEAK} under the full energy peak determined for the same live time of the multichannel analyser. The ratio N_{OUT}/N_{IN} versus N_{IN} represents the general throughput of the linear electronics. The ratio N_{PEAK}/N_{IN} gives the proportion of events of interest.

The number of counts N_{IN} and N_{OUT} are determined using two scalers which measure respectively the count rate of TC245 ICR pulses and the count rate at the output of the linear electronics.

The dead times of Tennelec TC245 BDC, Intertechnique 7201 gated integrator and Ortec 675 Ge resolution enhancer modules are controlled by their respective pile-up rejector circuits. Thus, their throughput characteristics depend on the different designs of pile-up rejector.

Throughput

The throughput characteristics represented by the N_{OUT}/N_{IN} ratio plotted versus N_{IN} are shown in fig.6 for different ballistic deficit correctors and shaping time constants (2 μs, 1 μs and 0.5 μs). All the data are normalised in such a way that the values measured at 3000 counts/s with the triangular shaping at 2 μs and 1 μs shaping time and with the TC245 BDC at 0.5 μs shaping time are equal to one. No background correction has been applied. Statistical and systematical uncertainties lead to error bars of about 1.5 % and 1 % at respectively low and high count rate. As the numbers N_{IN} and N_{OUT} are determined by two independent discriminators whose thresholds differ slightly, an additionnal inaccuracy of about 2-3 % is introduced. According to the general throughput trend, a systematical improvement of the throughput is observed for all electronic modules with shortened shaping time constants. Let us compare the different ballistic deficit correctors.

First of all a much higher throughput is observed with the amplifier alone, since this module is not controlled by a pile-up rejector. TC245 BDC is comparable to both the 7201 gated integrator and 675 Ge resolution enhancer at respectively 0.5 μs and 1 μs shaping times and 2 μs shaping time.

Based on the curves presented in fig.6, the average dead time ΔT of the different linear electronics are calculated using the following equation [11]:

$$N_{OUT}/N_{IN} = e^{-N_{IN}\Delta t} \qquad (1)$$

The deduced values are given in table 3. The dead time determined for the amplifier alone corresponds to the peaking time T_p quoted for the TC245 triangular pulse (Tp = 2.4 C where C is the amplifier shaping time) plus the stretcher contribution ($\sim 1\mu$s). The dead times of the ballistic deficit correctors represent their pile-up inspection times. Table 3 reflects a difference between the design of the the TC245 BDC pile-up rejector and those of the 675 Ge resolution enhancer and 7201 gated integrator modules. The latter two exhibit about 10 % and 25% longer

pile-up inspection times respectively. The conclusion that the TC245 amplifier in the standard mode shows a much higher throughput than the other electronic modules is strongly modified if the full energy peak efficiency versus input count rate is considered.

Full energy peak throughput

The full energy peak efficiency of the four Ge detectors was measured with a ^{60}Co source. The number of counts N_{PEAK} under the 1.33 MeV full energy peak was determined by the multichannel analyser working in the live time mode and applying an automatic background subtraction. The N_{PEAK}/N_{IN} ratios were deduced versus N_{IN}. There was no connection between the different pile-up rejector modules and the ADC.

At low count rates ($\leq$ 10000 counts/s), the N_{PEAK}/N_{IN} values are sensitive to two effects. The laboratory background is no longer negligible due to the large detection efficiency of the Ge counters. It artificially increases N_{IN} which, in turn, reduces the N_{PEAK}/N_{IN} ratio. Thus the input count rates have been corrected by the background contribution, about 340 counts/s, measured at the TC245 ICR output without source.

The second effect was discovered after completion of the measurements. Typically, measurements as a function of count rate are performed by changing the geometry between the source and the detector. At low count rate, the source is far from the detector and close to the floor whereas at high count rate the geometry is reversed. For energy resolution measurements this setup is quite satisfactory. Looking to N_{PEAK}/N_{IN} ratios, however, one can expect distortions associated with the γ-rays scattering from the floor. Again the data obtained at low count rates are the most affected. To estimate the floor scattering contribution, additional measurements have been performed in two steps. First the detector is in the same geometry (setup DOWN) as in the throughput measurements whereas in the second step it is placed far from any dense material (setup UP). Background and ^{60}Co source spectra were recorded in both geometries for the same duration in the live time mode. In the setup DOWN, the source was placed on the floor and corresponded to about 1000 ICR pulses per second. The 1.33 MeV peak areas were used to normalise the UP and DOWN data. After background subtraction,

the difference between the UP (N_U) and DOWN(N_D) number of counts gives the floor contribution (N_F). If f corresponds to the proportion of N_D counts due to the floor scattering, it is defined as:

$$f = N_F/N_U \qquad \text{with} \quad N_D = N_U(1+f) \tag{2}$$

and equals 0.7. Analysing the floor-source-detector geometry during the throughput measurements and taking into account the f factor representing the probability for the γ-rays emitted in the direction of the floor to be backscattered into the Ge crystal, we deduce the floor correction that is to be applied.

Fig.7 plots N_{PEAK}/N_{IN} ratios appropriately corrected for laboratory background and floor scattering versus N_{IN} which were measured with the different ballistic deficit correctors at 2 μs, 1 μs and 0.5 μs shaping times. Note that the curve distortions around 20000 counts/s at 1 μs shaping time and around 10000 counts/s at 0.5 μs shaping time already existed before correction for the floor contribution.

Fig.7 shows that despite the large throughput of the TC245 amplifier alone compared to the other electronic modules (see fig.6) its full energy peak throughput is strongly reduced by pile-up (triangles). On contrary the TC245 working in the BDC mode exhibits excellent performance (full circles) which is close to that of the amplifier alone especially at 1 μs shaping time. Due to their longer pile-up inspection time, the 675 Ge resolution enhancer (stars) and the 7201 gated integrator (diamonds) show a smaller throughput, particularly the latter module at 1 μs shaping time.

It is interesting to note that the full energy peak throughput of the amplifier alone at 2 μs shaping time is still the largest of the tested electronic modules. As the TC245 in the standard mode is not controlled by the pile-up rejection, it seems that there is a number of events in which a second pulse overlaps the tail of the first one without introducing distortion of both peak amplitudes. Such an event, rejected by the standard pile-up rejectors, is taken as a valid event in the case of the amplifier alone and improves its full energy peak throughput. The pile-up rejector circuit of the Tennelec TC245 unit has an option which allows to take into account the events mentioned above. Although the throughput response of the TC245 BDC using that option has not been tested in the course of this work,

the performance of the unit should be improved with respect to fig.7 leading to a good compromise between energy resolution and throughput.

Peak-to-total ratio

The excellent throughput of the Tennelec TC245 unit working in the standard mode (fig.7) suggests to plot an additional quantity, N_{PEAK}/N_{OUT} versus N_{IN}, which corresponds to a fundamental characteristic of Ge spectrometers, the peak-to-total ratio [1-4]. In principle, this parameter should be constant for a given detector, a property approximately observed with TC245 BDC at 0.5 μs shaping time. Note again that the previous remarks concerning the background distortions at low count rate fully apply here. Thus the N_{PEAK}/N_{OUT} ratio was calculated using N_{PEAK}/N_{IN} and N_{OUT}/N_{IN} ratios, both quantities according to figs. 6 and 7 respectively. In this way two corrections were applied, the first one for background events affecting the N_{PEAK}/N_{IN} ratio at low count rate and the second one to compensate the poor relative adjustment of the ICR pulse and output pulse discriminator thresholds (normalisation of N_{OUT}/N_{IN} ratios at 3000 counts/s).

The ratio N_{PEAK}/N_{OUT} is plotted versus N_{IN} in fig.8. For the amplifier alone (triangles), it strongly and continuously decreases with count rate at both 2 μs and 1 μs shaping times. This shows the disadvantage of working without pile-up rejection. Indeed, the throughput remains artificially high (see triangles in fig.6) whereas the full energy peak throughput is strongly reduced by pile-up (see triangles in fig.7). The pile-up contributes in the energy spectrum to the high energy background which could hinder the obervation of γ-ray lines correlated to rare nuclear events such as superdeformation, exotic nuclear shapes, etc ....

At 0.5 μs shaping time, the N_{PEAK}/N_{OUT} values obtained with TC245 BDC are almost constant. Their average value, 0.123 (5) agrees very well with the peak-to-total value of about 0.280 measured with this type of Ge detector for both the 1.17 MeV and 1.33 MeV ^{60}Co peaks. Note the unexpected increase versus count rate of N_{PEAK}/N_{OUT} ratios for the TC245 BDC (full circles) at 2 μs and 1 μs shaping times and for the 675 Ge resolution enhancer (stars) at 2 μs shaping time.

The response of the 7201 gated integrator is much worse compared to the TC 245 BDC especially at 1 μs shaping time (diamonds). This is related to the design of its pile-up rejector which is fully efficient only when its inhibit output is

connected to the ADC [12]. This was not the case in our tests. When a pile-up event is recognised by the pile-up rejector circuit, the charge integration is blocked. A short and not completely integrated pulse is sent to the ADC which should be inhibited. In our measurements, such events which do not contribute to N_{PEAK} are still accounted in N_{OUT} leading to the observed downsloping curve.

The observed increase versus N_{IN} of the N_{PEAK}/N_{OUT} ratio at 2 μs shaping time for the Tennelec (full circles) and Ortec (stars) units does not result from an inaccuracy of the MCA live time mode which determines the duration of the measurements. The input count rate of the ADC is much lower at 2 μs shaping time (up to $\sim$ 20 000 counts/s) than that at 0.5 μs (up to $\sim$ 40 000 counts/s). Therefore to better understand this effect one has to reffer to the experimental conditions. The number of counts N_{OUT} is measured at the output of the pile-up rejector circuit and therefore is controlled by the pile-up rejector dead time. The N_{PEAK} value is given by the MCA which count rate is controlled by both linear electronics dead time (pile-up rejector dead time) and MCA dead time. The latter is compensated in the live time mode by the correction of the measurement duration. A comparison of the curves ploted for 0.5 μs, 1 μs and 2 μs shaping times suggests that the excess of the N_{PEAK}/N_{OUT} values is correlated with the pile-up rejector dead time. The shorter the shaping time, the smaller the excess. In fact, when a pulse is being treated by the linear electronics, any following pulse is accepted only after the pile-up inspection time. However as the first pulse is being encoded by the ADC after the peaking time, the MCA live time correction compensates for missed pulses during the trailing tail of the linear electronics, pulses which due to the pile-up rejector never enter the input of the ADC. This leads to an overcorrection by the multichannel analyser which artificially increases N_{PEAK}.

The above discussion covering the different throughput characteristics, N_{OUT}/N_{IN}, N_{PEAK}/N_{IN} and N_{PEAK}/N_{OUT}, clearly shows the superior performances of the Tennelec TC245 unit working in the BDC mode compared to the TC245 in the standard mode, the Intertechnique 7201 gated integrator and Ortec 675 Ge resolution enhancer. Taking into account its good energy resolution versus count rate this module is, at present, the best choice for high count rate experiments. Unfortu-

nately the Ortec 973 high rate amplifier equipped with a gated integrator could not be tested whereas the 7201 unit is only a first generation module of this type. For low and moderate count rates, below 10 000 counts/s the Ortec 675 Ge resolution enhancer is also very attractive because of its excellent energy resolution and quite high throughput.

In order to have a general overview of the electronics performances versus count rate for both energy resolution and throughput, we propose a synthetic representation in fig.9 which plots the FWHM measured for the 1.33 MeV full energy peak versus one of the throughput ratios (N_{OUT}/N_{IN} in our case). Each point corresponds to a definite count rate. For a perfect unit without deterioration with count rate of either the energy resolution or the throughput, all points would be stacked at the bottom (small FWHM) right-hand side ($N_{OUT}/N_{IN} \sim 1$) of the figure as a single point. If only throughput varies with input rate, the module performances appear as a horizontal line (see 675 Ge resolution enhancer). On the contrary, if only the FWHM is sensitive to N_{IN}, the figure shows a vertical line. The better the electronics module, the shorter the curve and the closer it lies to the bottom right-hand side of the figure.

Fig.9 shows that at 0.5 μs shaping time the 7201 gated integrator exhibits larger FWHM and throughput spreads than the TC245 BDC. Especially its energy resolution varies considerably with count rate. At 1 μs shaping time the gated integrator has a slightly better energy resolution, except at 50000 counts/s, than the TC245 BDC with, however, a smaller throughput. Finally at 2 μs shaping time the TC245 in the standard mode (Triang.) has the larger throughput (short curve) with a poor average FWHM ($\sim$ 2.4 keV) whereas the 675 Ge resolution enhancer gives the best energy resolutions ($\sim$ 2.0 keV) balanced however by a large throughput reduction (long horizontal curve) versus N_{IN}. TC245 BDC shows intermediate performances (FWHM $\sim$ 2.2 keV and a slightly smaller throughput spread than the 675 unit).

Thus the Tennelec TC245 module working in the BDC mode leads to satisfactory performances over the whole 0.5-2 μs shaping time range. Taking into account the easy preliminary adjustment of the pile-up rejector, this module is very useful for large γ-ray multidetector arrays. Despite the long time (about 10 min) necessary to optimise the ballistic deficit corrector parameters to each Ge

counter, the Ortec 675 Ge resolution enhancer is a good tool for low count rate experiments requiring excellent energy resolution.

3.2.2. Comparison of the detectors

In principle, the throughput characteristics of the different electronics modules should be independent of the detector used. The linear electronics dead time corresponds to the peaking time in the case of the linear amplifier alone and to the pile-up inspection time in the case of ballistic deficit correctors. This is confirmed by fig.10 which presents the throughput N_{OUT}/N_{IN} versus the input count rate for the three detectors 40219, 40187 and 30526. The three curves are practically superimposed within the error bars (about 2-3 %).

In contrast, the N_{PEAK}/N_{IN} versus N_{IN} data depend on the detector used since it is strongly correlated with the peak-to-total ratio. Fig.11 presents N_{PEAK}/N_{IN} ploted versus input count rate for a triangular shaping at 2 μs shaping time and for the TC245 BDC at 1 μs and 0.5 μs shaping times. Note that, with a good accuracy, the two detectors 40219 and 40187 are equivalent and show almost identical N_{PEAK}/N_{IN} ratios from 5000 to 50000 counts/s. The same type of data for detector 30526 differs significantly. At low count rate, the N_{PEAK}/N_{IN} ratio is comparable to the values obtained with the other tested detectors. At higher count rates, however, the curve is shifted down, reflecting smaller N_{PEAK} values. In addition, this detector presents a serious deterioration of the energy resolution versus count rate, (see sect. 3.1.2. and fig.5). This FWHM degradation results from the large tail on the right-hand side of the full energy peak. No doubt part of the events under this tail are subtracted from those under the full energy peak.

This further confirms the conclusion of sect. 3.1.2. which stresses that it is not sufficient to characterise detectors only by characteristics measurements at low count rates ($\sim$ 1000 counts/s).

4. Conclusions

The comparative study of different ballistic deficit correction methods carried out with four large Ge detectors of about 70 % relative efficiency versus input count rate (from 3 to 50 kcounts/s) shows that for spectroscopy systems working

with short shaping time constants ($\leq$ 2 μs) the best compromise between energy resolution and electronics throughput is achieved with Tennelec TC245 linear amplifier working in the ballistic deficit correction (BDC) mode. The energy resolution obtained with this module based on the Hinshaw method varies by less than 0.35 keV over the whole count rate range. The pile-up inspection time is the shortest of the tested units for all shaping times, especially at 1 μs shaping time, leading to a full energy peak throughput similar to that of the TC245 amplifier alone working without pile-up rejection.

For low and moderate input count rates ($\leq$ 10 kcounts/s) the Ortec 675 Ge resolution enhancer module based on the Goulding/Landis method offers at 2 μs shaping time an excellent energy resolution with a quite high throughput. This unit corrects for both ballistic deficit and carrier trapping leading to FWHM values almost insensitive ($\sim$ 0.15 keV) to count rate.

The Intertechnique 7201 gated integrator unit exhibits large energy resolution variations ($\sim$ 0.5 keV) and a lesser throughput as compared to the TC245 BDC. This module, however, is not the last generation of gated integrators and to complete the study of this correction method, the Ortec 973 high rate amplifier equipped with a gated integrator should be tested.

Finally the Tennelec TC245 linear amplifier working in triangular shaping allows at 2 μs shaping time quite reasonable energy resolutions ($\sim$ 2.4 keV) without ballistic deficit correction for a large throughput.

A new throughput representation has been proposed which summarises in a single plot the energy resolution and throughput versus count rate. Such synthetical figures are useful for comparing different electronics modules.

This work has underlined that sum-peaks, which are quite broad lines with conventional linear amplifiers, appear as symmetrical and narrow single lines after ballistic deficit correction. This effect points out the effectiveness of the correction circuits which, in turn, complicates the analysis of rare events in high-rate data spectra.

The analysis of the Ge detector energy resolution versus count rate using different ballistic deficit correctors and shaping time constants is a good tool to investigate Ge crystal quality. Indeed, we have shown that detector 30526, which at 1000 counts/s and at 6 μs shaping time presents quite good performances, has a

large external dead layer. It is also interesting to notice that this counter shows the smallest carrier trapping of the four detectors tested which leads to a fundamental question: do the surface treatments or contact preparation processes generate trapping centers close to the external surface of Ge crystals ?

For throughput studies, care should be taken to avoid an overcorrection for counts due to the multichannel analyser working in the live time mode.

Acknowledgements

The authors acknowledge the different manufacturers (Ortec, Tennelec and Intertechnique) who provided the NIM modules for ballistic deficit correction that were used in this work.

References

[1] F.A.Beck, Prog. Part. Nucl. Phys. 28 (1992)443;

C.W.Beausang et al., Nucl. Instr. and Meth. A313 (1992) 37.

[2] D.Bazzacco, Proc. Int. Conf. on Nuclear Structure at High Angular Momentum, Ottawa, AECL10613, Vol.2 , 1992, p.376.

[3] I.Y.Lee, Nucl. Phys. A520 (1990) 641 c.

[4] J.Gerl and R.M.Lieder (eds.), EUROBALL proposal, GSI Darmstadt, 1991.

[5] J.Alexander, I.Lazarus, G.M.McPherson, E.C.G.Owen, F.A.Beck, C.Ring, Ch.Ender, J.Pouxe and A.Richard, IEEE Trans. Nucl. Sci NS-39(4) (1992) 886.

[6] B.W.Loo, F.S.Goulding and D.Gao, IEEE Trans. Nucl. Sci. NS-35(1988)114.

[7] M.Moszyński and G.Duchêne, Nucl. Instr. and Meth. A308 (1991)557.

[8] S.M.Hinshaw and D.A.Landis, IEEE Trans. Nucl. Sci. NS-37(2) (1990) 374.

[9] F.S.Goulding and D.A.Landis, IEEE Trans. Nucl. Sci. NS-35 (1988)119.

[10] M.L.Simpson, T.W.Raudorf, T.J.Paulus and R.C.Trammell, IEEE Trans. Nucl. Sci NS-36(1989)260.

[11] R.D.Evans, The Atomic Nucleus (McGraw-Hill Book Company, New York 1955).

[12] Intertechnique 7201 gated integrator manual.

Figure Captions

Fig.1. Spectra of the 1.33 MeV ^{60}Co line measured with the Ortec Ge detector 40219 at low (3000 counts/s) and high (50000 counts/s) count rate with different amplifying systems. (a) Tennelec TC245 linear amplifier with a triangular shaping; (b) Tennelec TC245 BDC linear amplifier in ballistic deficit correction mode; (c) Tennelec TC245 linear amplifier connected to the Ortec 675 Ge resolution enhancer; spectra (a), (b) and (c) were obtained with a 2 μs shaping time constant; (d) Tennelec TC245 BDC linear amplifier in ballistic deficit correction mode; (e) Tennelec TC245 linear amplifier connected to the Intertechnique 7201 gated integrator (GI); spectra (d) and (e) were obtained with a 1 μs shaping time constant.

Fig.2. Energy resolution at 1.33 MeV versus input count rate measured with detector 40219 for different amplifying systems and different shaping time constants. Tennelec TC245 linear amplifier with a triangular shaping at 2 μs shaping time (triangles), in BDC mode at 2 μs, 1 μs and 0.5 μs shaping times (full circles), connected to Ortec 675 Ge resolution enhancer at 2 μs shaping time (stars) and connected to an Intertechnique 7201 gated integrator at 1 μs and 0.5 μs shaping times (diamonds).

Fig.3. Spectra of the 662 keV ^{137}Cs line (left-hand side) and of the 1324 keV ^{137}Cs sum-peak (right-hand side) measured with detector 40219 at 2 μs shaping time and at 37000 counts/s in different conditions. (a) Tennelec TC245 linear amplifier with a triangular shaping, (b) with the pile-up rejector switched on and (c) in BDC mode.

Fig.4. Energy resolution at 1.33 MeV versus input count rate measured with four Ortec Ge detectors 40187 (stars), 40228 (diamonds), 40219 (full squares) and 30526 (full circles) at 2 μs and 1 μs shaping times with different amplifying systems: Tennelec TC245 linear amplifier with triangular shaping (Triang.) and in the BDC mode for both shaping times, connected to Ortec 675 resolution enhancer at 2 μs shaping time and connected to Intertechnique 7201 gated integrator at 1 μs shaping time

Fig.5. Spectra of the 1.33 MeV ^{60}Co line measured with detector 30526, Tennelec TC245 linear amplifier in the BDC mode and 2 μs shaping time. Front irradiation at 3000 counts/s (a) and at 50000 counts/s (b). Side irradiation at 50000 counts/s (c).

Fig.6. Linear electronics throughput, represented by the ratio of the number of output pulses to the number of input pulses, versus input count rate measured with detector 40219 at different shaping time constants. The different linear amplifying systems used are: Tennelec TC245 linear amplifier with a triangular shaping at 2 μs and 1 μs shaping times (triangles), in the BDC mode at 2 μs, 1 μs and 0.5 μs shaping times (full circles), connected to Ortec 675 Ge resolution enhancer at 2 μs shaping time (stars) and connected to Intertechnique 7201 gated integrator at 1 μs and 0.5 μs shaping times (diamonds).

Fig.7. Same as fig.6 for the full energy peak throughput represented by the ratio of the number of counts in the 1.33 MeV ^{60}Co line to the number of input pulses.

Fig.8. Same as fig.6. for the peak-to-total throughput represented by the ratio of the number of counts in the 1.33 MeV ^{60}Co line to the number of output pulses.

Fig.9. Energy resolution at 1.33 MeV, measured with detector 40219 at different shaping time constants, versus linear electronics throughput and input count rate. The latter ranging from 3 to 50 kcounts/s is represented by different symbols. Data have been obtained using the Tennelec TC245 linear amplifier with a triangular shaping at 2 μs shaping time (Triang.), in the BDC mode at 2 μs, 1 μs and 0.5 μs shaping times (BDC), connected to Ortec 675 Ge resolution enhancer at 2 μs shaping time (675) and connected to an Intertechnique 7201 gated integrator at 1 μs and 0.5 μs shaping times (GI). The lines are drawn to guide the eye.

Fig.10. TC245 BDC throughput versus input count rate measured with the Ge detectors 40187 (stars), 40219 (full squares) and 30526 (full circles) at 1 μs shaping time.

Fig.11. Full energy peak throughput versus input count rate measured with the Ge detectors 40187 (stars), 40219 (full squares) and 30526 (full circles) and

Tennelec TC245 linear amplifier with a triangular shaping at 2 μs shaping time and in the BDC mode at 1 μs and 0.5 μs shaping times.

Table 1

Ortec Ge detector specifications

Detector	30526	40219	40187	40228
Dimensions				
diameter [mm]	73.0	71.6	72.8	72.3
length [mm]	72.5	72.4	77.7	69.4
Bias voltage [V]	- 3500	- 4500	- 3000	- 4000
Resolution ^{60}Co [keV][a)]	1.97	1.98	2.11	1.92
Peak shape ^{60}Co (FWTM/FWHM)	1.97	1.88	1.88	1.88
Peak-to-Compton ratio ^{60}Co	70.4	77.7	73.5	78.0
Resolution ^{57}Co [eV]	840	775	814	729
Relative efficiency ^{60}Co [%]	68.0	73.0	80.6	74.3

[a)] FWHM measured with a 6 μs shaping time constant and Gaussian shaping.

Table 2

Tested electronics and shaping time constants

Shaping time constants [μs] (Triangular amplifier pulses)	
TC245	1, 2
TC245 BDC	0.5, 1, 2
TC245 +7201	0.5, 1
TC245 + 675	2

Table 3

Linear electronics dead times given in μs. The accuracy of these values varies from 0.1 μs for the smallest to 0.3 μs for the largest.

shaping time	0.5 μs	1 μs	2 μs
Triang.		3.0	5.2
BDC	3.1	7.5	14.5
GI	4.1	8.7	
675			15.8

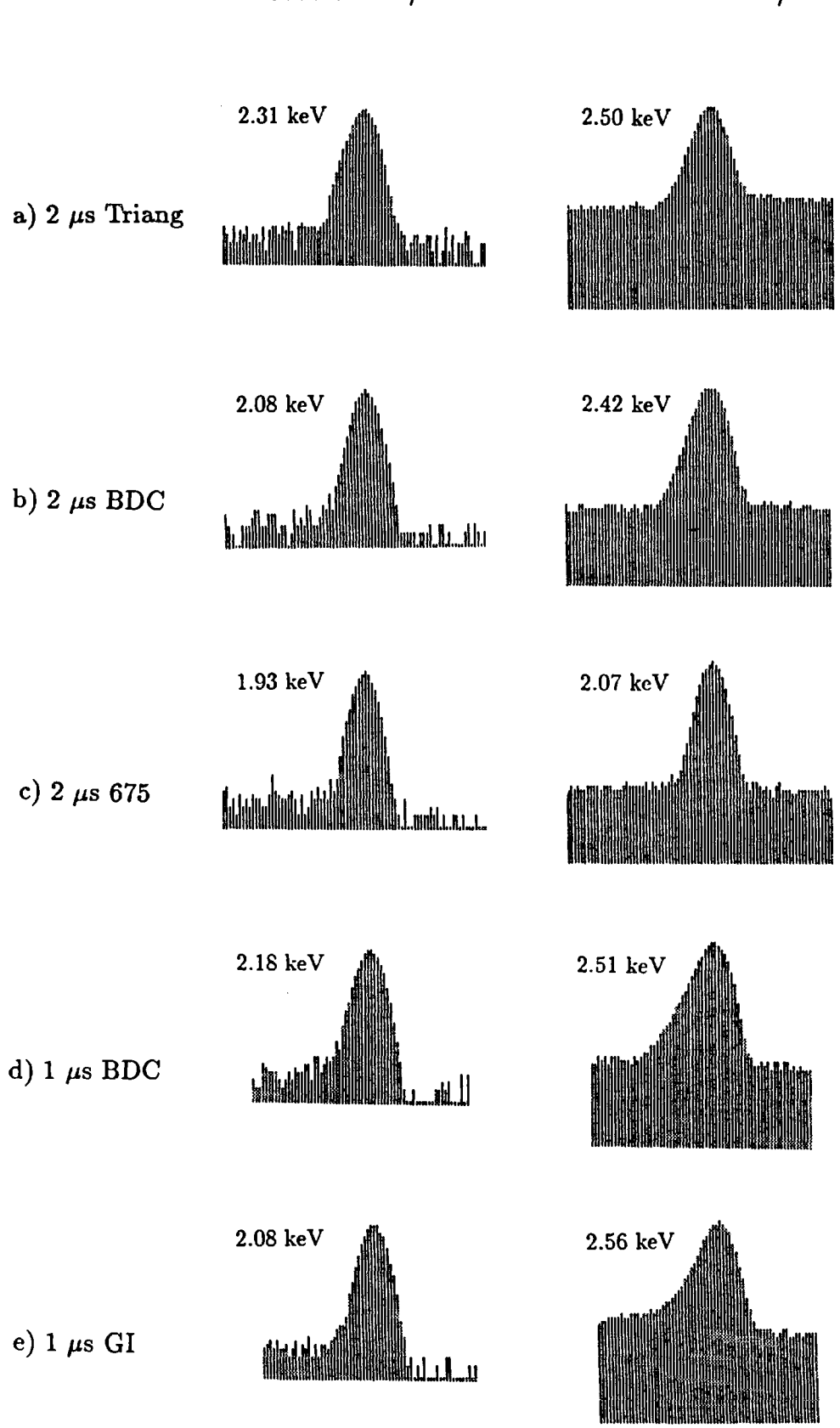
3000 counts/s
50 000 counts/s
a) 2 μs Triang
2.31 keV
2.50 keV
b) 2 μs BDC
2.08 keV
2.42 keV
c) 2 μs 675
1.93 keV
2.07 keV
d) 1 μs BDC
2.18 keV
2.51 keV
e) 1 μs GI
2.08 keV
2.56 keV

Figure 1

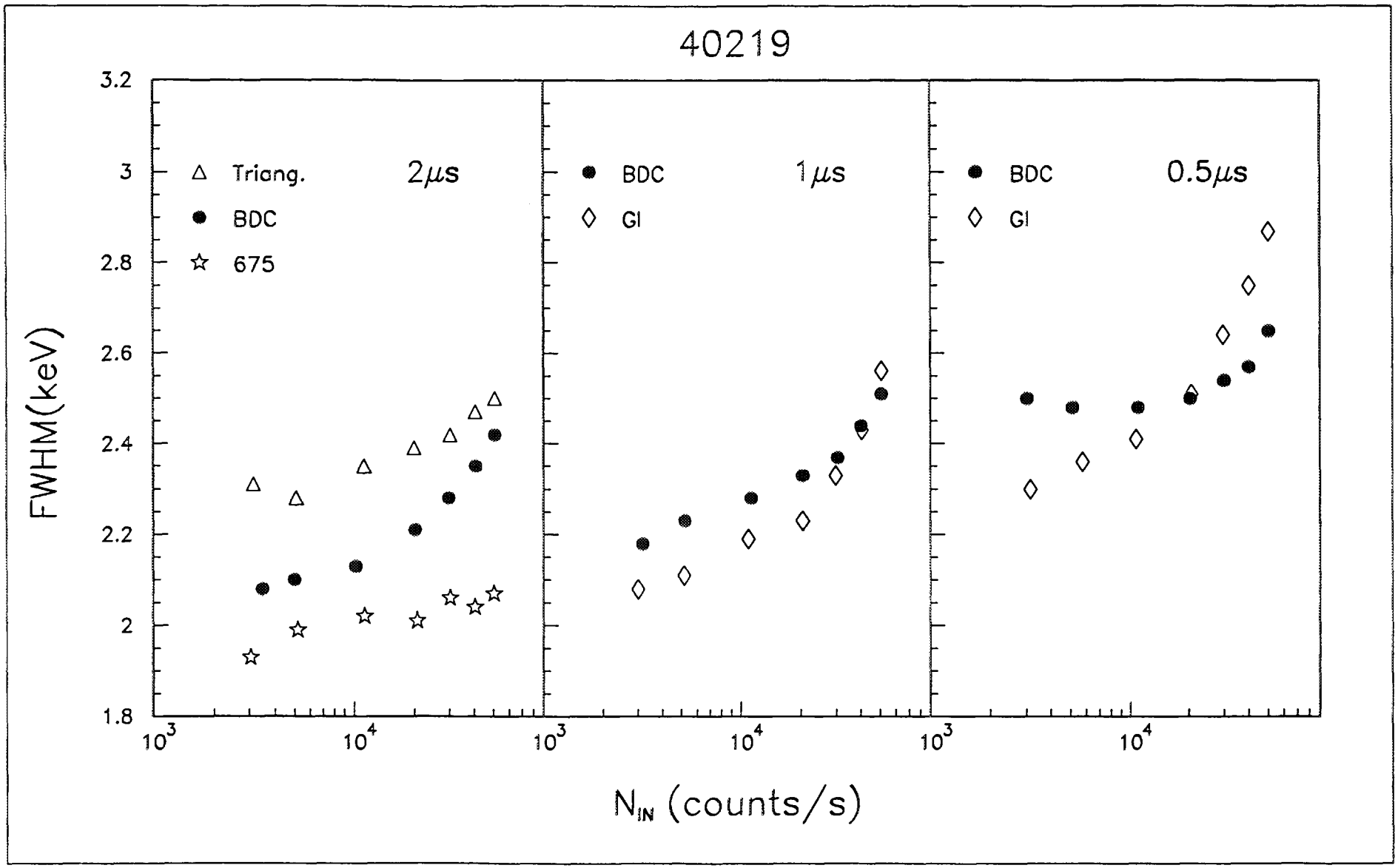
40219
FWHM(keV)
3.2
3
2.8
2.6
2.4
2.2
2
1.8
Triang.
BDC
675
2μs
BDC
GI
1μs
BDC
GI
0.5μs
10^3
10^4
N_IN (counts/s)

Figure 2

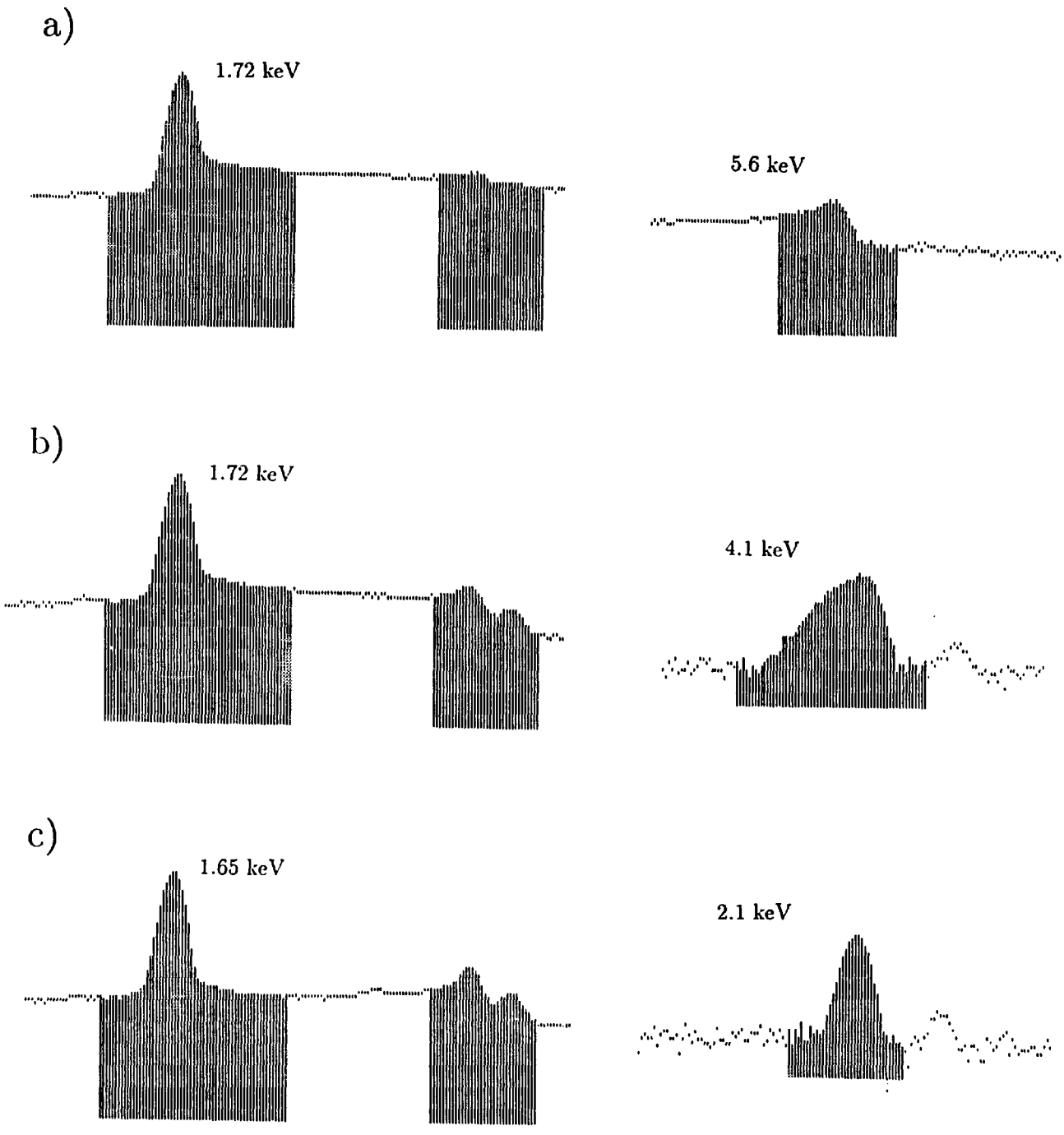

Figure 3

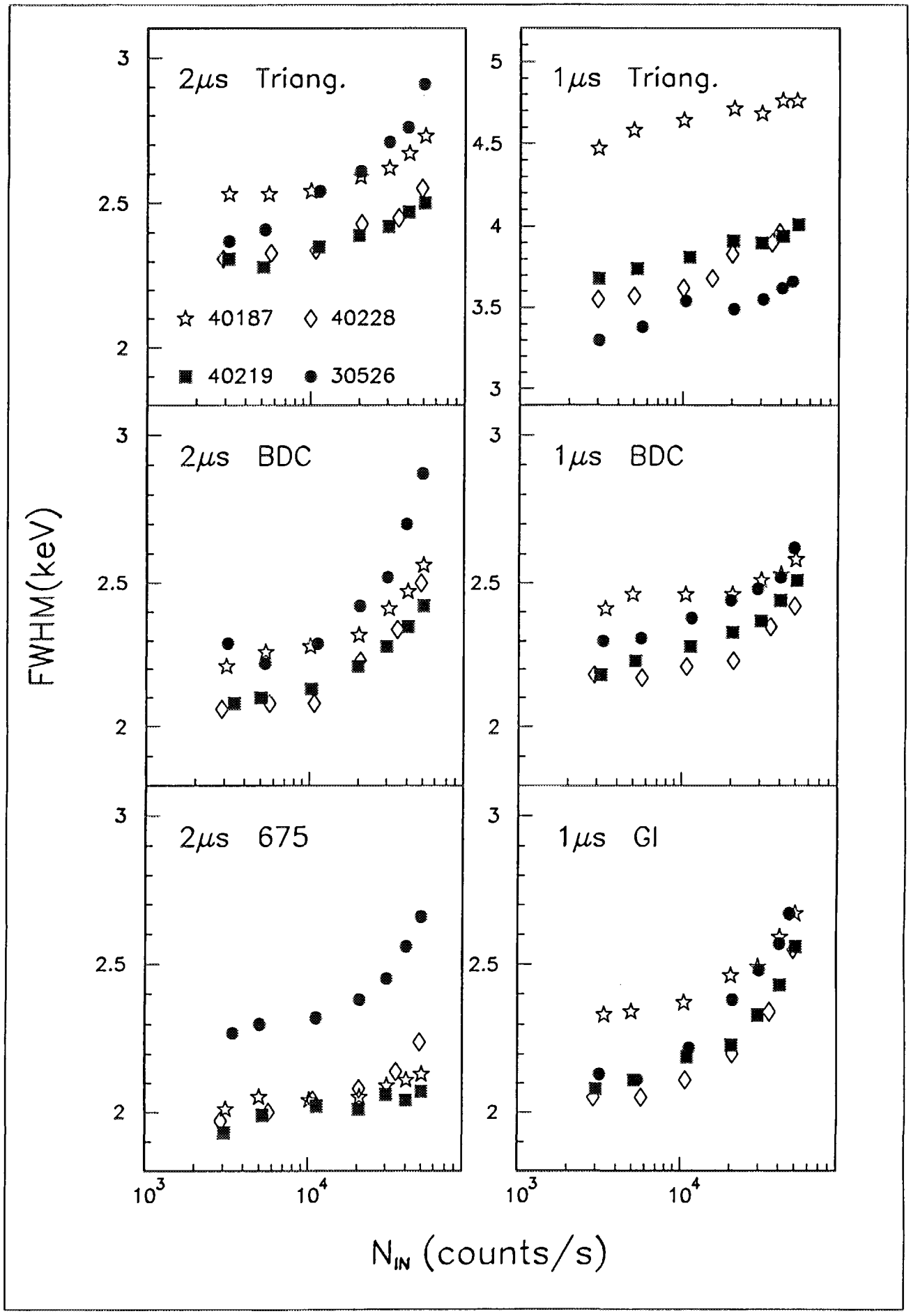
2μs Triang.
1μs Triang.
2μs BDC
1μs BDC
2μs 675
1μs GI
40187
40228
40219
30526
FWHM(keV)
N_IN (counts/s)

Figure 4

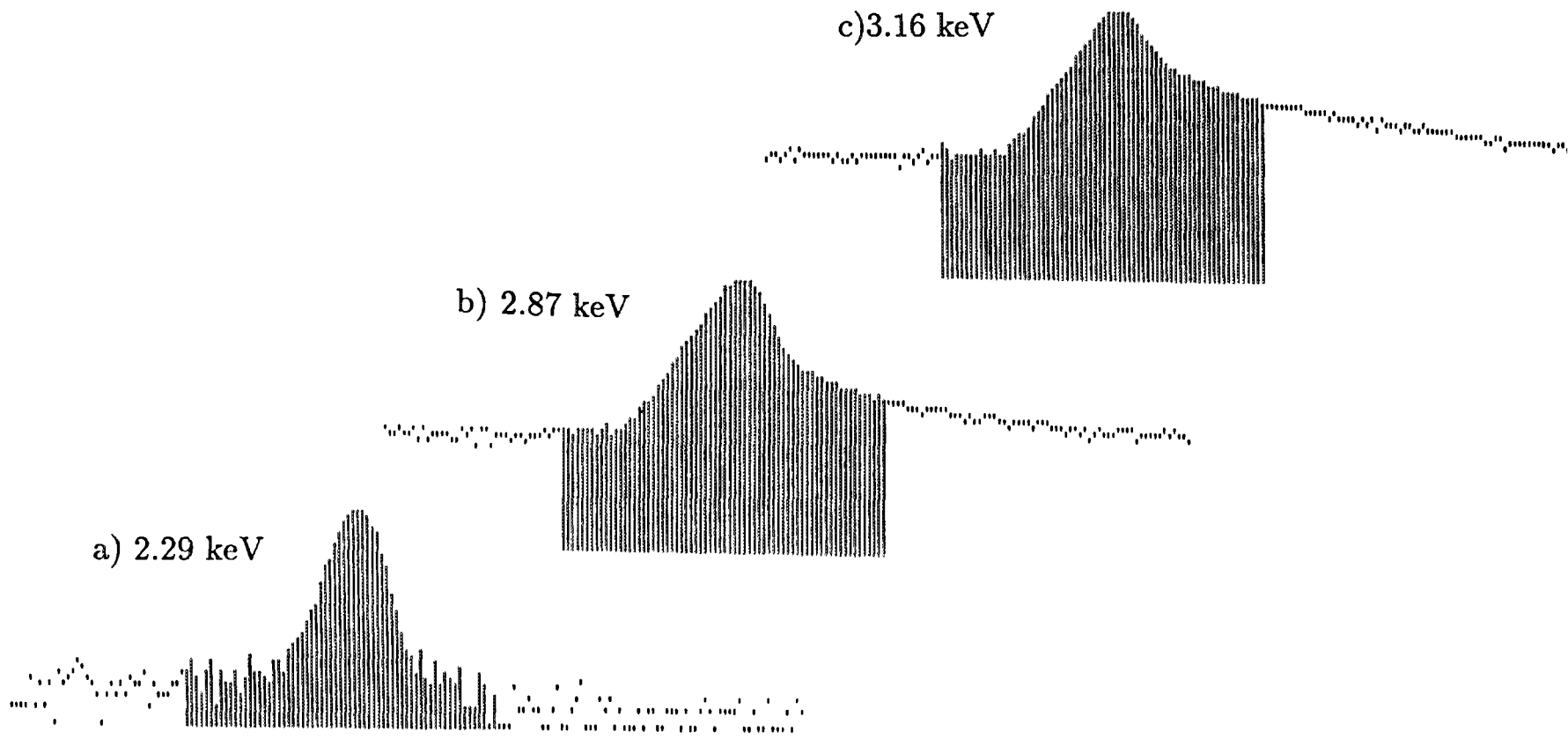

Figure 5

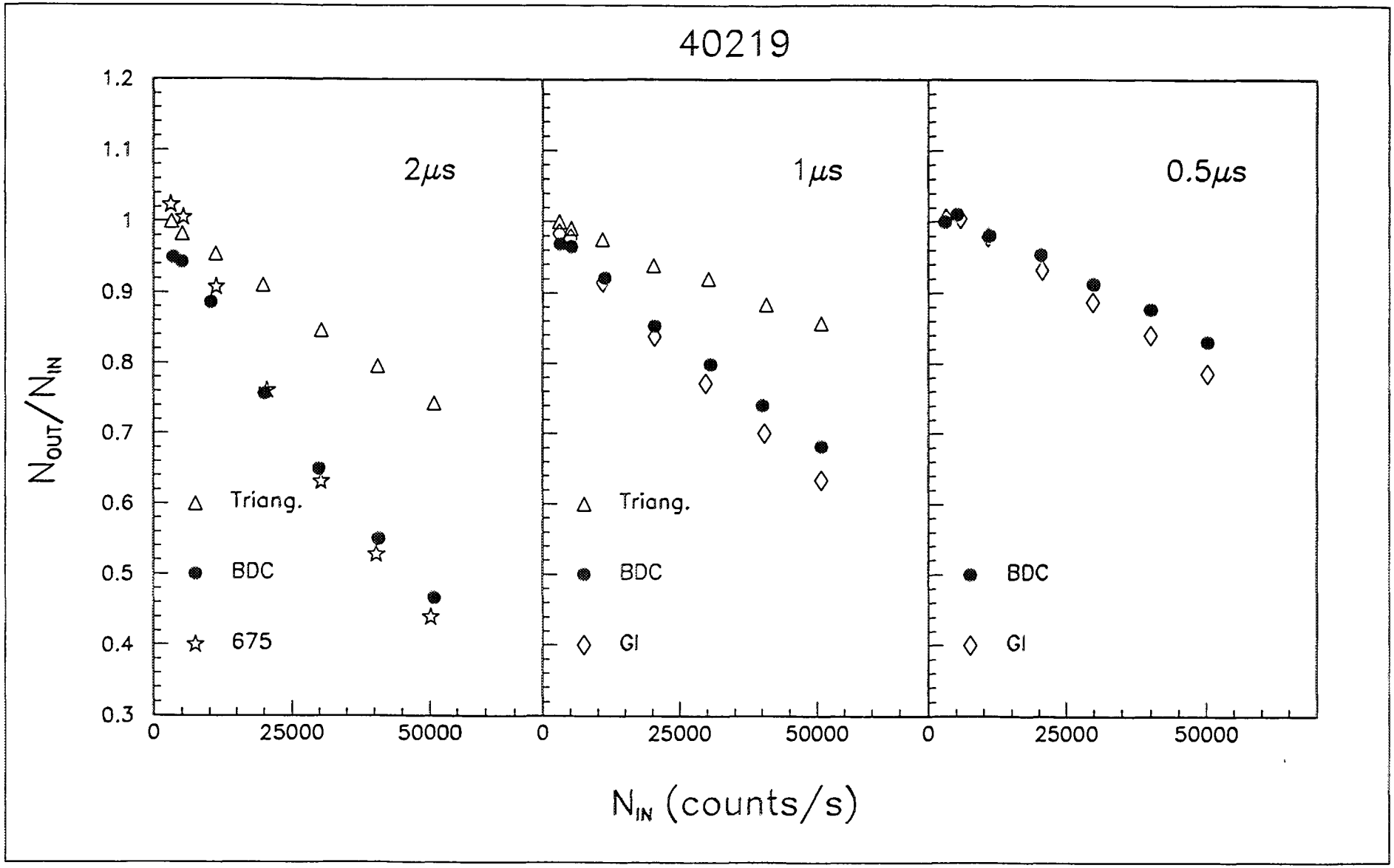
40219
2μs
1μs
0.5μs
Triang.
BDC
675
Triang.
BDC
GI
BDC
GI
N_{OUT}/N_{IN}
N_{IN} (counts/s)
1.2
1.1
1
0.9
0.8
0.7
0.6
0.5
0.4
0.3
0
25000
50000

Figure 6

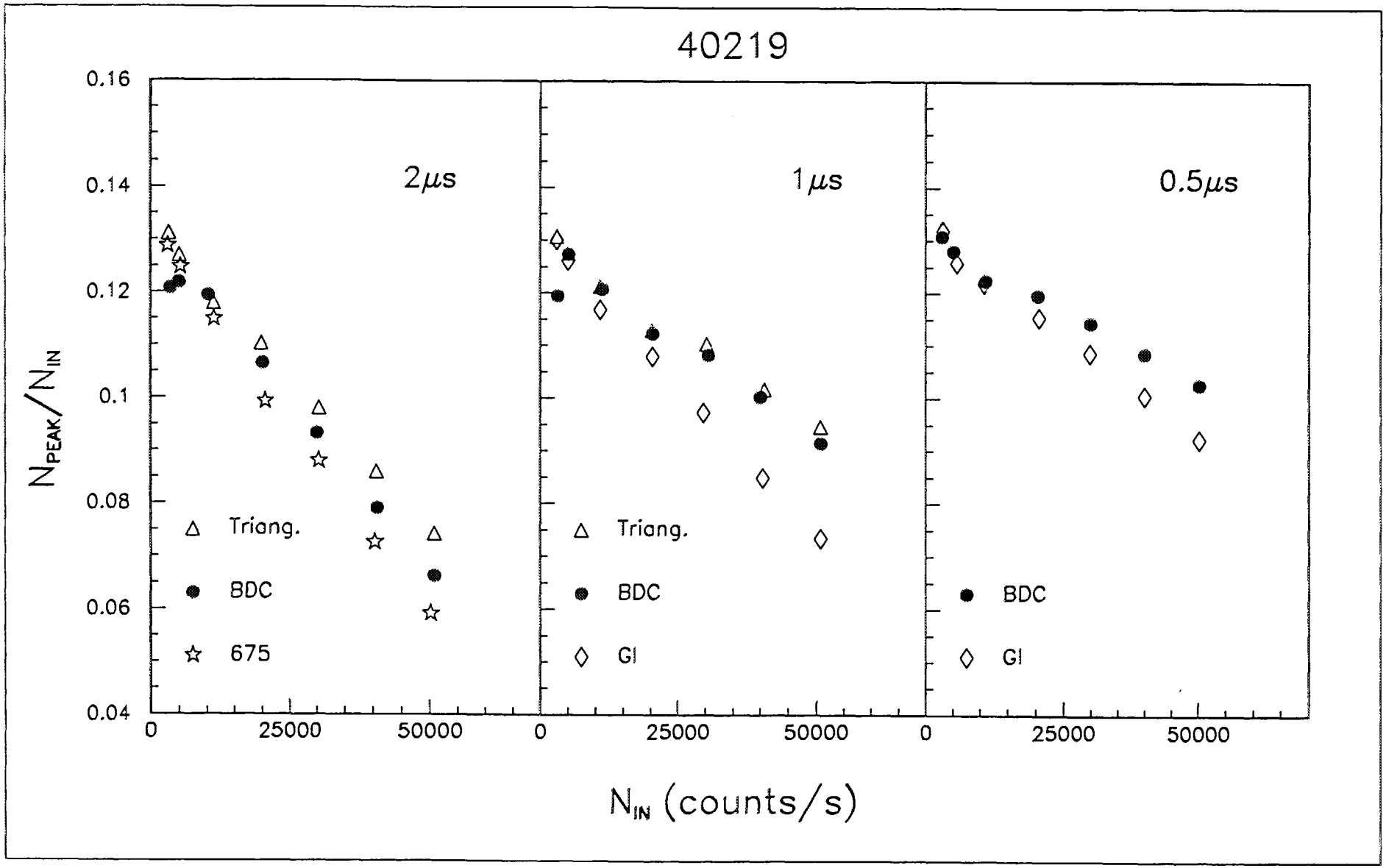
40219
2μs
1μs
0.5μs
0.16
0.14
0.12
0.1
0.08
0.06
0.04
N_{PEAK}/N_{IN}
Triang.
BDC
675
Triang.
BDC
GI
BDC
GI
0
25000
50000
N_{IN} (counts/s)

Figure 7

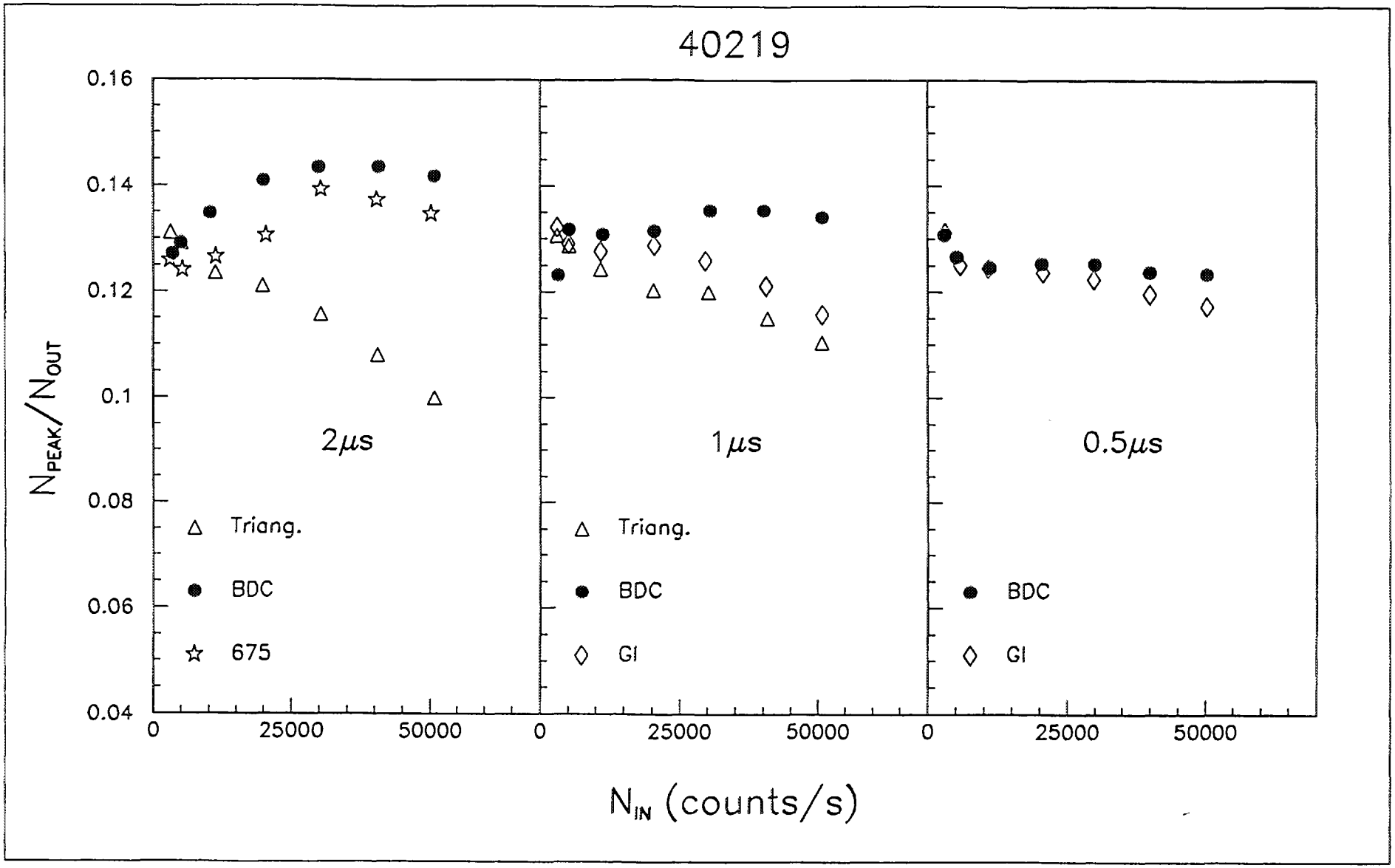
40219
0.16
0.14
0.12
0.1
0.08
0.06
0.04
N_{PEAK}/N_{OUT}
2μs
1μs
0.5μs
Triang.
BDC
675
Triang.
BDC
GI
BDC
GI
0
25000
50000
0
25000
50000
0
25000
50000
N_{IN} (counts/s)

Figure 8

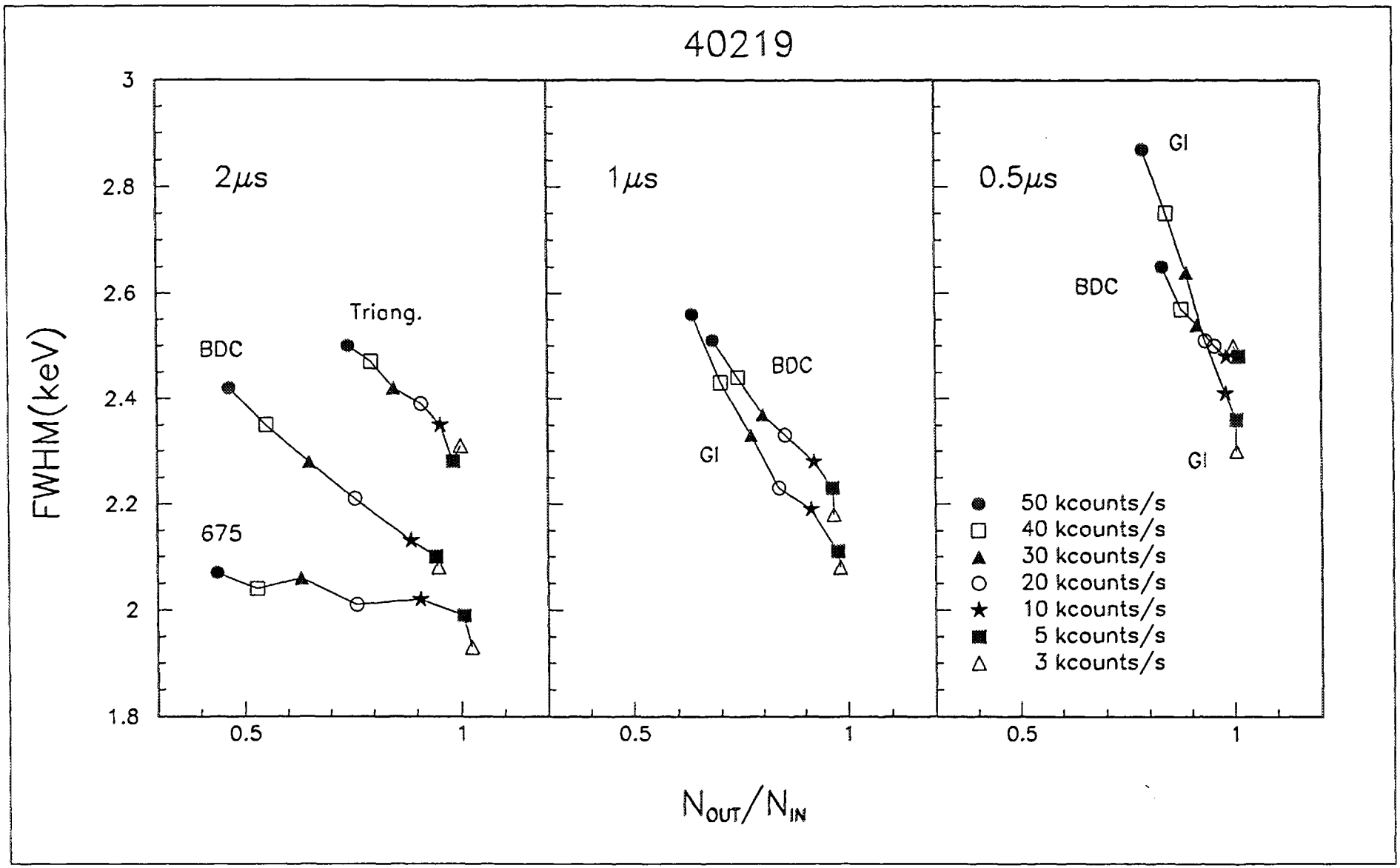
40219
FWHM(keV)
3
2.8
2.6
2.4
2.2
2
1.8
2μs
1μs
0.5μs
Triang.
BDC
675
BDC
GI
GI
BDC
GI
50 kcounts/s
40 kcounts/s
30 kcounts/s
20 kcounts/s
10 kcounts/s
5 kcounts/s
3 kcounts/s
0.5
1
0.5
1
0.5
1
N_OUT/N_IN

Figure 9

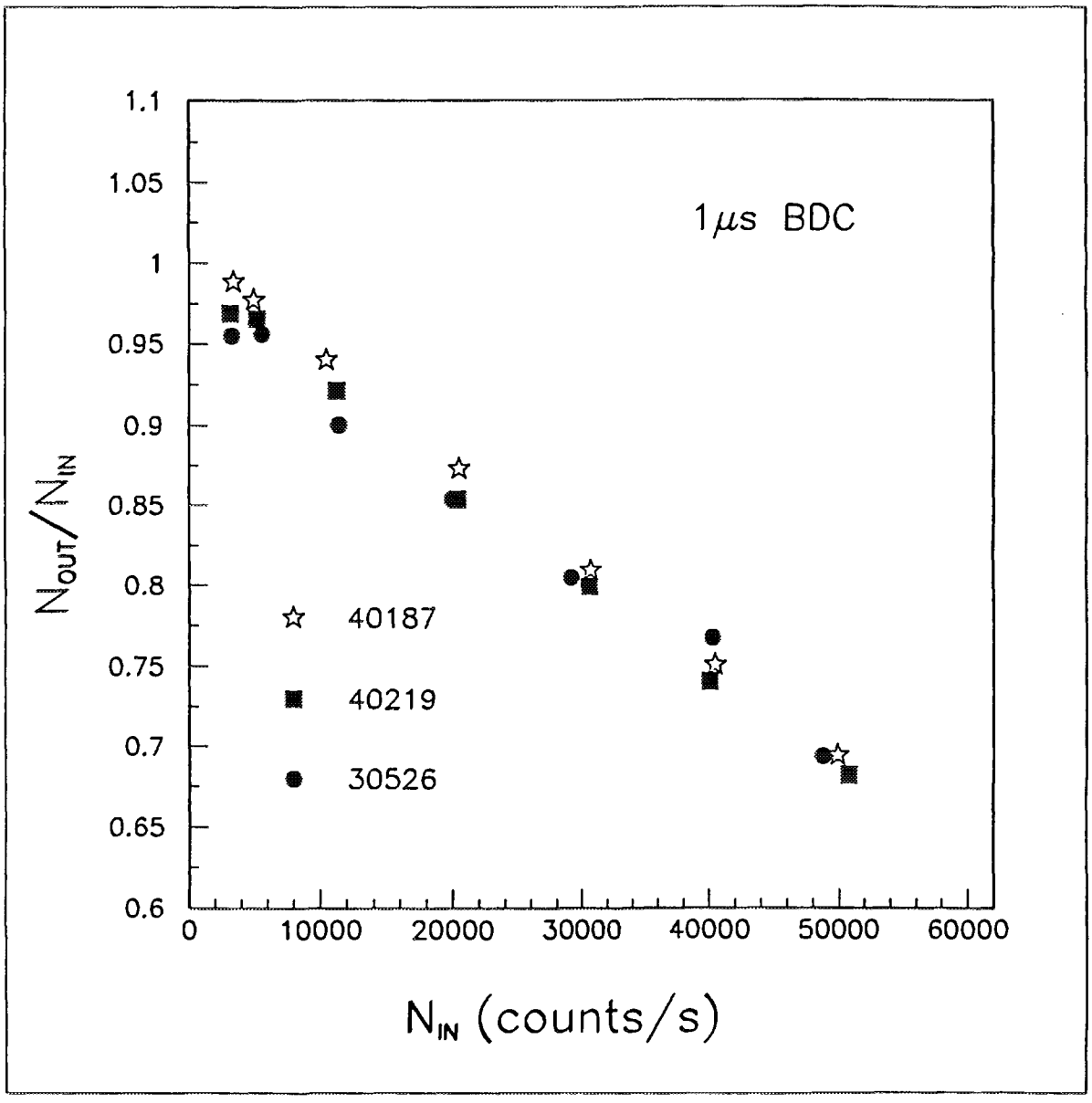
1.1
1.05
1
0.95
0.9
0.85
0.8
0.75
0.7
0.65
0.6
0
10000
20000
30000
40000
50000
60000
N_{OUT}/N_{IN}
N_{IN} (counts/s)
1μs BDC
40187
40219
30526

Figure 10

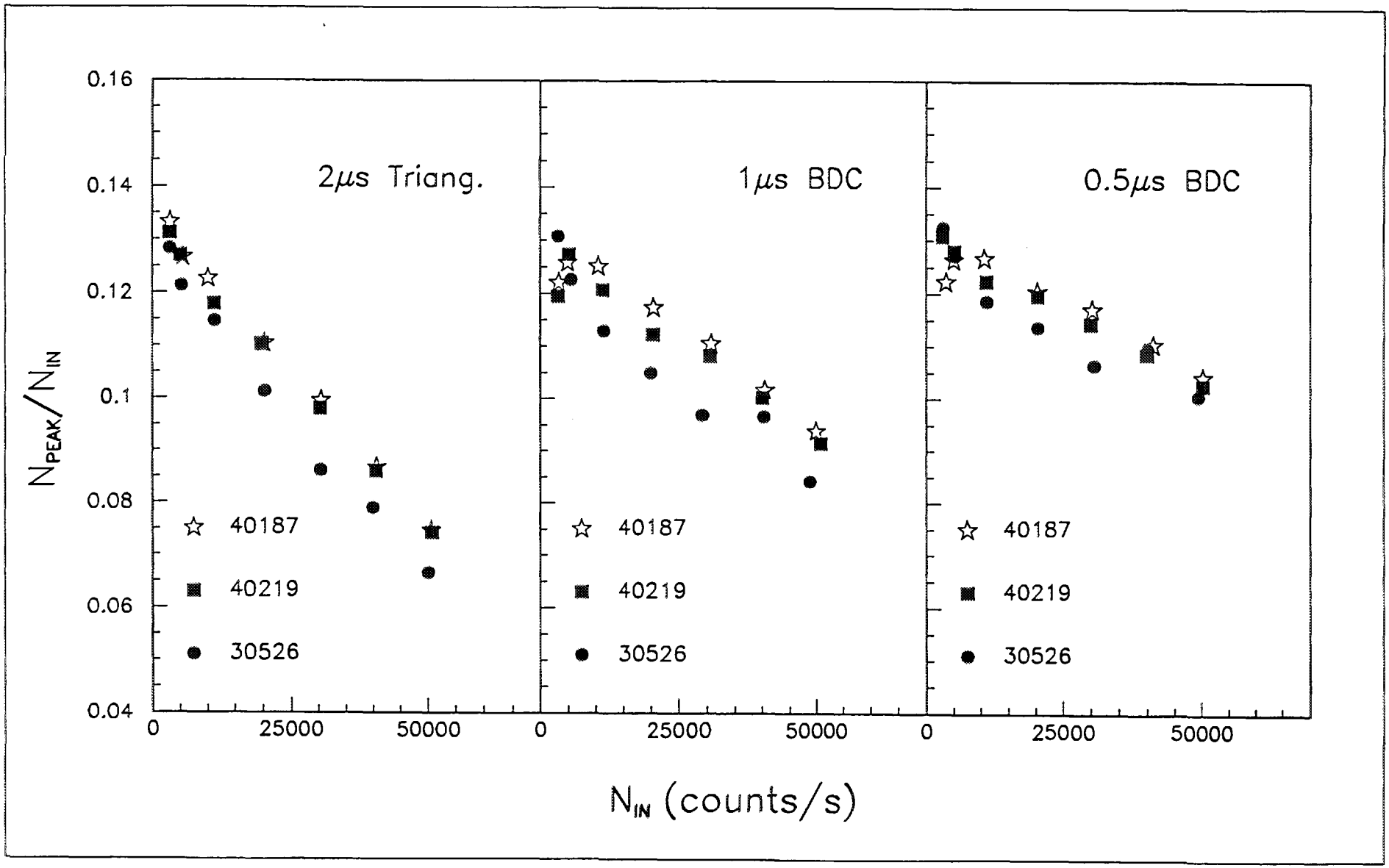
0.16
0.14
0.12
0.1
0.08
0.06
0.04
N_{PEAK}/N_{IN}
2μs Triang.
1μs BDC
0.5μs BDC
40187
40219
30526
0
25000
50000
N_{IN} (counts/s)

Figure 11